

# **Multi-layered holograms and their fabrication**

VOLODYMYR M. FITIO

National University Lvivska Polytechnica, 12 S. Bandery Str., 79013 Lviv, Ukraine.

YAROSLAV V. BOBITSKI

National University Lvivska Polytechnica, 12 S. Bandery Str., 79013 Lviv, Ukraine.  
Institute of Technics, Rzeszów University, ul. Rejtana 16A, 35-959, Rzeszów, Poland.

Multi-layered holograms due to their multi-beam interference have other features contrary to usual bulk holograms. Analysis of the properties of such holograms is provided by coupled waves method. For two-layered holograms we can see oscillations of the dependence of diffraction efficiency on an angle incident onto a hologram or on the wavelength of incident beam, and besides oscillation period is defined mainly by the distance between holograms. Multi-layered holograms could be presented as two-dimensional periodic structures, for which variable of the dielectric constant (variable component of refractive index) could be shown as multiplication of two periodical functions.

## **1. Introduction**

For the first time, analysis of multi-layered holograms was provided in [1] on the basis of Kogelnik diffraction [2]. In this work, analytical dependence of diffraction efficiency of multi-layered holograms is described and some of their properties presented. A theory concerning thin two-layered holograms and their properties is also provided in [3], [4]. Results of theoretical investigations of multi-layered holograms registered on photo-refractive materials are given in paper [5]. But previous theoretical investigations were based on the Kogelnik theory of light diffraction on bulk holograms [2]. This theory is approximate and thus it describes a simple thick hologram, but there is no certainty that it is applicable to theoretical model creation of multi-layered holograms, as presented in [1], because of neglecting the second derivative. Based on the coupled modes theory for light diffraction on periodical structures [6], a system of exact differential equations was obtained without the second derivative being neglected, which was used for analysis of thick holograms [7]. Using this system of equations we performed digital analysis of multi-layered holograms [8] by solving the system with the Runge–Kutta method of the fourth order, taking into consideration the second derivative and for a parabolic approximation [6]. A comparison of calculation

results of exact equations and those for a parabolic approximation shows that they are similar. This is not surprising, because calculations were made for small modulation of refractive index of hologram medium under the following condition:

$$\frac{2n_1}{\lambda} Tm \leq 1 \quad (1)$$

where:  $n_1$  is the amplitude of refractive index modulation,  $T$  – thickness of one hologram,  $m$  – number of holograms in multi-layered hologram,  $\lambda$  – wavelength of incident beam. So, fulfilling condition (1), which is easy to do in practice, we can use parabolic approximation and obtain the analytical dependence of diffraction efficiency on an incident angle and on the wavelength of beam incident onto multi-layered hologram and on other parameters of such a hologram. It is also necessary to analyse the properties of multi-layered holograms and indicate their possible application. Whereas two-layer holograms are easy to fabricate on the basis of photopolymeric composites [8], fabrication of multi-layered holograms, especially for large  $m$  ( $> 10$ ), could bring about some technological difficulties. Therefore, the question arises whether it is possible to fabricate multi-layered holograms for large  $m$ , using, exceptionally, holographic process, which for this case is more acceptable.

## 2. Theoretical analysis of multi-layered holograms

Let relative permittivity into the first sub-hologram, with the thickness  $T$ , of multi-layered hologram (Fig.1) change in the following way:

$$\varepsilon(x, y, z) = \begin{cases} \varepsilon_a, & -\infty < z < 0, & T < z < T + d, & -\infty < x < \infty \\ \varepsilon_a + \varepsilon_1 \cos\left(\frac{2\pi}{\Lambda}x\right), & 0 \leq z \leq T, & -\infty < x < \infty \end{cases} \quad (2)$$

where:  $\Lambda$  is the period of change along the  $OX$  axis,  $\varepsilon_a$  – permittivity constant of medium besides sub-hologram,  $\varepsilon_1$  – the amplitude of variable component of permittivity constant of sub-hologram,  $d$  – distance between two neighbouring sub-holograms. Permittivity constant of other holograms changes the same way.

If a plane wave of one-amplitude electric field falls on such a hologram at an angle  $\theta_0$ , then, besides incident wave, there also appear diffracted waves. It is well known from the theory of diffraction on thick holograms [2], [6] that in many cases it is sufficient to consider only two coupled waves, diffracting at zero and first orders at angles  $\theta_0$  and  $\theta_1$ , respectively. Let us limit the problem to consideration of an optical wave, the electric field tension of which is orthogonal to the plane of incidence. The electric field in a hologram is presented in the following way [6], [7]:

$$E(x, z) = \sum_{i=0}^{\pm} A_i(z) \frac{1}{\sqrt{\cos\theta_i}} \exp[-j(k_{i,x}x + k_{i,z}z)] \quad (3)$$

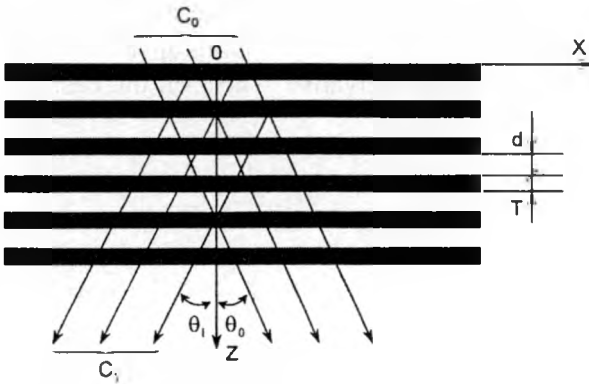


Fig. 1. General view of multi-layered hologram, where wide black lines are sub-holograms with the thickness  $T$  at a distance  $d$  to each other.

where:  $A_i(z)$  are amplitudes of non-diffracted ( $i = 0$ ) or diffracted ( $i = 1$ ) waves in hologram,  $k_{i,x}, k_{i,z}$  – the projections of wave vectors onto  $OX$  and  $OZ$  axes, respectively.

Substituting Eq. (3) into the second order wave equation [6], [9] for electric field in which dielectric penetration is shown as Eq. (2), then, according to a procedure given in papers [6] and [7], we obtain the following system of differential equations:

$$\begin{cases} \frac{d^2 A_0}{dz^2} - 2jk_{0,z} \frac{dA_0}{dz} + a \sqrt{\frac{\cos\theta_0}{\cos\theta_1}} A_1 \exp(-j\Delta z) = 0, \\ \frac{d^2 A_1}{dz^2} - 2jk_{1,z} \frac{dA_1}{dz} + a \sqrt{\frac{\cos\theta_1}{\cos\theta_0}} A_0 \exp(j\Delta z) = 0. \end{cases} \quad (4)$$

where:

$$a = k^2 \frac{n_1}{n_0}, \quad n_0 = \sqrt{\epsilon_a}, \quad n_1 = \frac{\epsilon_1}{2n_0}, \quad k^2 = k_i^2 = \left(\frac{2\pi n_0}{\lambda}\right)^2.$$

Difference of two projections of wave vectors onto  $OZ$  axis plays an important part for our problem

$$\Delta = k_{1,z} - k_{0,z}. \quad (5)$$

The diffraction angle  $\theta_1$  is defined by condition approved in [7]

$$\frac{2\pi}{\Lambda} + k_{1,x} - k_{0,x} = 0. \quad (6)$$

It is well known that for considering the light diffraction on thick holograms when  $n_1 \ll n_0$ , parabolic approximation is applied [6], and the essence of this approximation is that the system of Eqs. (4) neglects the second derivative. Then, on the basis of system (4) by changing the variables

$$A_0 = C_0 \exp\left(-j\frac{\Delta}{2}z\right),$$

$$A_1 = C_1 \exp\left(j\frac{\Delta}{2}z\right),$$

we obtain the linear system of differential equations with constant coefficients:

$$\begin{cases} \frac{dC_0}{dz} = j\frac{\Delta}{2}C_0 - j\chi C_1, \\ \frac{dC_1}{dz} = -j\chi C_0 - j\frac{\Delta}{2}C_1. \end{cases} \quad (7)$$

Besides, the coefficient connecting both equations of the system equals

$$\chi = \frac{a}{2k\sqrt{\cos\theta_0\cos\theta_1}}.$$

It is worth mentioning that the system of Eqs. (7) describes also propagation of both waves between sub-holograms, but in this case  $\chi = 0$ , and the system (7) splits into two independent equations. The period  $\Lambda$  is defined at the stage of hologram recording correspondingly to the correlation [2], [10]

$$\frac{2\pi}{\Lambda} = \frac{4\pi n_0}{\lambda_0} \sin\varphi \quad (8)$$

where:  $\varphi$  is the angle of laser beam propagation in a medium upon hologram recording (the scheme of recording is symmetrical),  $\lambda_0$  – wavelength of laser irradiation upon hologram recording. In the following equation  $\varphi$  and  $\lambda_0$  will also mean the wavelength and the angle of beam propagation in the hologram, respectively, for which Bragg conditions are satisfied. Using Eqs. (6) and (8) we can define the angle of diffraction  $\theta_1$  on the hologram for the stipulated wavelength  $\lambda$  and the incident angle  $\theta_0$

$$\sin\theta_1 = 2\frac{\lambda}{\lambda_0} \sin\varphi - \sin\theta_0. \quad (9)$$

Taking angle  $\theta_1$  defined by formula (9) and based on expression (5) we can calculate  $\Delta$

$$\Delta = \frac{2\pi n_0}{\lambda} [\cos\theta_1 - \cos\theta_0]. \quad (10)$$

Using the theory of linear differential equations [11] and matrix calculation [11], [12], amplitudes of electric fields of non-diffracted and diffracted waves for  $z = T + d$  could be written as matrix equation

$$\begin{bmatrix} C_0(T+d) \\ C_1(T+d) \end{bmatrix} = \begin{bmatrix} a_{11} & a_{12} \\ a_{21} & a_{22} \end{bmatrix} \begin{bmatrix} C_0(0) \\ C_1(0) \end{bmatrix} = \begin{bmatrix} a_{11} & a_{12} \\ a_{21} & a_{22} \end{bmatrix} \begin{bmatrix} 1 \\ 0 \end{bmatrix} \quad (11)$$

where  $C_0(0) = 1$  and  $C_1(0) = 0$  are initial conditions.

$$a_{11} = \exp\left(\frac{\Delta d}{2}i\right) \left[ \cos(\gamma T) + i \frac{\Delta}{2\gamma} \sin(\gamma T) \right], \quad a_{22} = a_{11}^*, \quad (12)$$

$$a_{12} = -i \frac{\chi}{\gamma} \sin(\gamma T) \exp\left(\frac{\Delta d}{2}i\right), \quad a_{21} = -a_{12}^*, \quad (13)$$

where  $\gamma = \sqrt{\left(\frac{\Delta}{2}\right)^2 + \chi^2}$ .

By direct checking using (12) and (13) we could prove the following:

$$\det(a_{ij}) = 1, \quad (14)$$

$$|a_{11}| = |a_{22}| \leq 1. \quad (15)$$

If multi-layered hologram consists of  $m$  sub-holograms, then the amplitude of electric field of both waves for  $z = m(T + d)$  taking into consideration (11) equals

$$\begin{bmatrix} C_0(mT + md) \\ C_1(mT + md) \end{bmatrix} = \begin{bmatrix} a_{11} & a_{12} \\ a_{21} & a_{22} \end{bmatrix}^m \begin{bmatrix} 1 \\ 0 \end{bmatrix} = \begin{bmatrix} b_{11} & b_{12} \\ b_{21} & b_{22} \end{bmatrix} \begin{bmatrix} 1 \\ 0 \end{bmatrix}. \quad (16)$$

From Eq. (16) it follows that the diffraction efficiency  $\eta$  of multi-layered hologram equals

$$\eta = |C_1(mT + md)|^2 = |b_{21}|^2. \quad (17)$$

From matrix calculation [11], [12] it is well-known that using conditions (14) and (15),  $b_{21}$  could be defined as follows:

$$b_{21} = a_{21} \frac{\sin(m\beta)}{\sin\beta} \quad (18)$$

where  $\beta$  is defined from formula

$$\cos\beta = 0.5(a_{11} + a_{22}) = \cos(\gamma T) \cos\left(\frac{\Delta d}{2}\right) - \frac{\Delta}{2\gamma} \sin(\gamma T) \sin\left(\frac{\Delta d}{2}\right). \quad (19)$$

From definition of  $a_{11}$  and  $a_{22}$  (formula (12)) it follows that  $|\cos\beta| \leq 1$ , and that is why  $\beta$  is real value. So, diffraction efficiency of multi-layered hologram taking into consideration (13), (17) and (18) equals

$$\eta = \frac{\chi^2}{\gamma^2} \sin^2(\gamma T) \frac{\sin^2(m\beta)}{\sin^2\beta}. \quad (20)$$

For  $m = 1$  (one-layer hologram) we obtain the well-known expression [2], [10], and for  $m = 2$  formula (20) becomes simpler, *i.e.*,

$$\eta = 4 \frac{\chi^2}{\gamma^2} \sin^2(\gamma T) \cos^2\beta. \quad (21)$$

It is easy to prove that if  $d = 0$  and  $m = 2$ , then  $\eta = \chi^2 \sin^2(2\gamma T) / \gamma^2$ , which is the diffraction efficiency of one-layer hologram with  $2T$ , according to [2], [10]. It is worth mentioning that formula (20) is analogous to corresponding equation in [1], although they are obtained in different ways.

### 3. Properties of multi-layered holograms

From the analysis of Eqs. (19), (20) it follows that in the case of  $d \gg T$ ,  $m = 2$  in the dependence of the diffraction efficiency  $\eta$  on the incident angle  $\theta_0$  at the definite wavelength  $\lambda_0$  (or in the dependence of  $\eta$  to  $\lambda$  at definite  $\varphi$ ) there appear brightly marked oscillations, the period of which is definite by  $\cos^2\beta$ . The period of oscillations could be evaluated from correlation (19). For  $\Delta \gg \chi$  (at large deviations from Bragg conditions)  $\cos\beta \cong \cos(T\Delta/2 + d\Delta/2)$ , and in the case of  $\Delta \ll \chi$  (at minimum deviations from Bragg conditions)  $\cos\beta \cong \cos(d\Delta/2)$ . In the first case ( $\Delta \gg \chi$ ) oscillation period is defined from formula  $(T + d)\delta(\Delta/2) = \pi$ , and, in the other case,  $d\delta(\Delta/2) = \pi$ . On the basis of formulae (9) and (10) at small deviations from Bragg angle it could be possible to define approximately  $\Delta_\lambda$  (wavelength of incident beam changes) and  $\Delta_\theta$  (incident angle changes), which equal to:

$$\Delta_\lambda \cong \frac{4\pi n_0}{\lambda_0^2} \tan(\varphi) \sin(\varphi) \Delta\lambda, \quad \Delta_\theta \cong \frac{4\pi n_0}{\lambda_0} \sin(\varphi) \Delta\theta_0. \quad (22)$$

Analogously, from correlations (22) for  $\Delta \ll \chi$  it follows that periods of oscillations upon the wavelength of incident beam changing and changing the angle incident onto the hologram equal

$$\delta(\Delta\lambda) \cong \frac{\lambda_0^2}{2dn_0 \tan \varphi \sin \varphi}, \quad \delta(\Delta\theta_0) \cong \frac{\lambda_0}{2dn_0 \sin \varphi}. \tag{23}$$

Let us define the periods of oscillations for wavelength  $\delta(\Delta\lambda)$  and for angle  $\delta(\Delta\theta_0)$  for the following conditions:  $\lambda_0 = 0.633 \mu\text{m}$ ,  $d = 10000 \mu\text{m}$ ,  $n_0 = 1.52$ ,  $\varphi = \pi/4$ . By consistent substitution of those data into formula (23), we obtain the following:  $\delta(\Delta\lambda) = 0.019 \text{ nm}$ ,  $\delta(\Delta\theta_0) = 2.94 \times 10^{-5} \text{ rad} = 0.1''$ . So, such a two-layered hologram has high selectivity with respect to angle of incidence of light beam and wavelength.

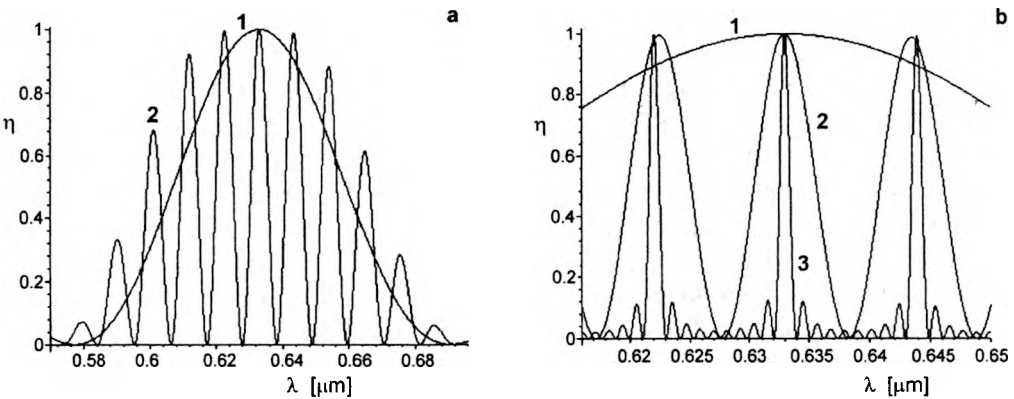


Fig. 2. Dependence of diffraction efficiency on wavelength for multi-layered holograms. 1, 2, 3 – one-layer, two- and ten-layered holograms, respectively.

Figure 2 shows dependences of diffraction efficiency on the wavelength of incident beam calculated with formula (21): for one-layer (curve 1) and two-layered (curve 2) holograms and ten-layered hologram (curve 3) under following conditions:  $\lambda_0 = 0.633 \mu\text{m}$ ,  $d = 100 \mu\text{m}$ ,  $T = 20 \mu\text{m}$ ,  $n_0 = 1.52$ ,  $\varphi = \pi/10$ ,  $\theta_0 = \pi/10$ ,  $n_1 m = 0.015$ . Along curve 2 oscillations and diffractive efficiency changes from zero to one at wavelengths approximately equal to Bragg wavelength are observed. Besides, maximum values of diffraction efficiency for two-layered hologram are higher than values of diffraction efficiency of one-layer hologram for the same wavelengths. For ten-layered hologram only the ninth peak has considerable amplitude and, furthermore, the widths of peaks for this hologram are considerably less than for two-layered hologram. For all holograms,  $n_1$  was selected such as to ensure that diffraction efficiency of holograms, when Bragg conditions are fulfilled, should equal 1.

Figure 3 shows dependences of diffraction efficiency on the wavelength for one-layer (curve 1), two-layered (curve 2) and one hundred-layered hologram

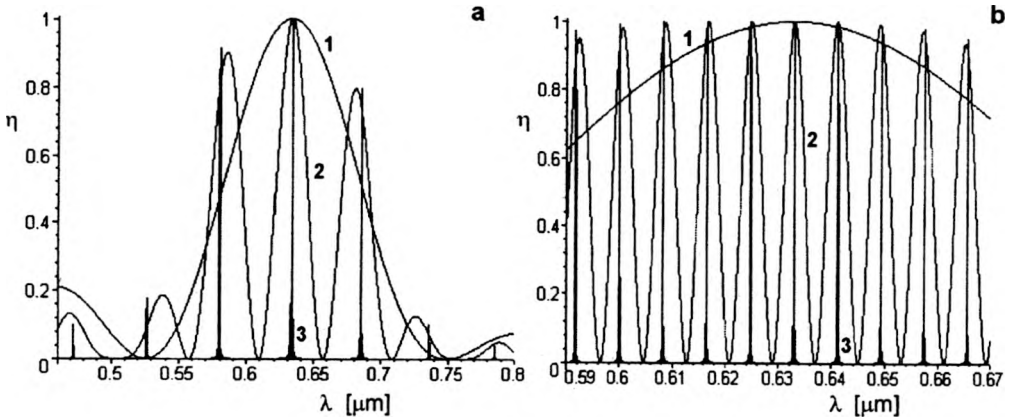


Fig. 3. Dependence of diffraction efficiency on wavelengths for multi-layered holograms. 1, 2, 3 – one-layer, two- and one hundred-layered hologram, respectively.

(curve 3) under the following conditions:  $\lambda_0 = 0.633 \mu\text{m}$ ,  $n_0 = 1.52$ ,  $\varphi = \pi/10$ ,  $\theta_0 = \pi/10$ ,  $n_1 m = 0.03$ . In Figure 3a:  $d = 15 \mu\text{m}$ ,  $T = 10 \mu\text{m}$ , and in Fig. 3b:  $d = 150 \mu\text{m}$ ,  $T = 10 \mu\text{m}$ .

Whereas the properties of multi-layered holograms, accordingly to Figs. 2 and 3 could, in general, be predictable without formula (21), the results of calculation of the envelope of diffraction efficiency for incident angle for two-layered hologram, as shown in Fig. 4, appear to be unpredictable. Curves 3 reflect the envelopes of oscillations of diffractive efficiency for incident angle for three wavelengths: 0.4, 0.6, 0.8  $\mu\text{m}$  at  $n_1 = 0.0092$ . From those curves it follows that if  $n_1 > n_{10}$  for every wavelength, at least for some interval  $\lambda < \lambda_{\text{max}}$ , then, there exist incident angles onto the hologram, which are relatively symmetric Bragg angles (for each wavelength), at

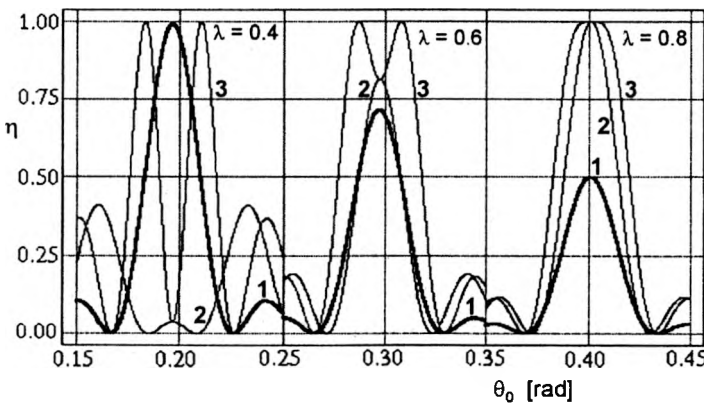


Fig. 4. Dependence of diffraction efficiency on incident angle for three wavelengths: 0.4, 0.6, 0.8  $\mu\text{m}$ : curve 1 – one-layer hologram,  $n_1 = 0.0092$ , curve 2 – one-layer hologram,  $n_1 = 0.0184$ , curve 3 – two-layered hologram,  $n_1 = 0.0092$ ,  $d = 5000 \mu\text{m}$ ,  $T = 20 \mu\text{m}$ .

which diffractive efficiency is close to unity. Connection between  $n_{10}$  and  $\lambda_{\max}$  is expressed by correlation which could be obtained from [10]

$$n_{10} = \frac{\lambda_{\max} \cos \varphi}{4T}$$

Curves 1 and 2 in Fig. 4 are plotted for comparison purposes and it is shown how diffraction efficiency for one-layer hologram depends on them. It follows that only upon execution of Bragg condition and at a defined value of  $n_1$ , for a given wavelength, diffraction efficiency equals one. The analysis of Figs. 2, 3 as well as formula (21) show that at large  $m = 10, 100$ , with diffraction efficiency depending on wavelength, narrow diffraction peaks appear at the expense of multi-beam interference.

This could be explained by that the multi-layered hologram could be presented as a periodic system, permittivity constant of which is described by the following expression:

$$\varepsilon(x, y, z) = \begin{cases} \varepsilon_a, & -\infty < z < 0, & m(T+d) < z < \infty, & -\infty < x < \infty, \\ \varepsilon_a + \varepsilon_1(z) \cos\left(\frac{2\pi}{\Lambda}x\right), & 0 \leq z \leq m(T+d), & -\infty < x < \infty. \end{cases} \quad (24)$$

Furthermore,  $\varepsilon_1(z)$  is a periodical function on coordinate  $z$  with period  $L = T + d$ . The periodicity of  $\varepsilon_1(z)$  explains the character of curves 3 in Figs. 2 and 3, because decomposition of  $\varepsilon_1(z)$  into Fourier series in correspondence with Fig.1 gives an infinite number of members, hence we have a large number of narrow peaks in the dependence of diffractive efficiency on wavelength or angle of beam incidence onto hologram.

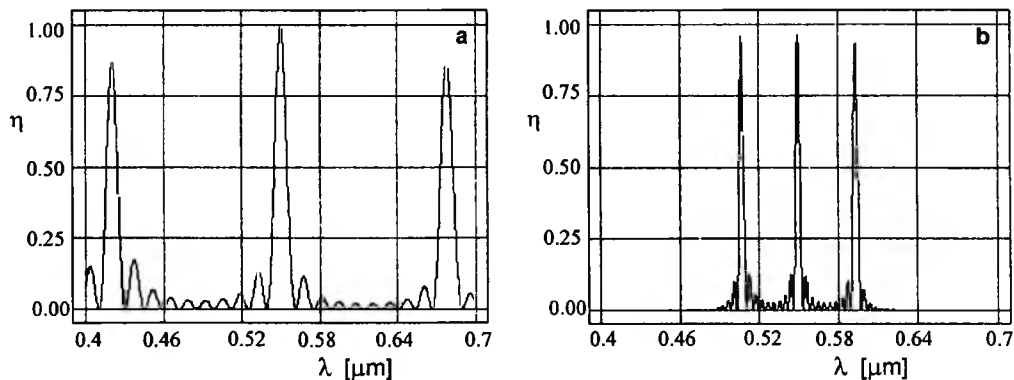


Fig. 5. Dependence of diffraction efficiency on wavelength when permittivity constant  $\varepsilon_1(z)$  is defined by Eq. (25). Total thickness of hologram: 250  $\mu\text{m}$ ,  $L = 25 \mu\text{m}$ ,  $n_{10} = 0.002$ ,  $n_{11} = 0.0011$  (a), and 750  $\mu\text{m}$ ,  $L = 75 \mu\text{m}$ ,  $n_{10} = 0.00067$ ,  $n_{11} = 0.00037$  (b).

If  $\varepsilon_1(z) = \varepsilon_{10} + \varepsilon_{11} \sin(2\pi z/L)$ , where:  $\varepsilon_{10}$  and  $\varepsilon_{11}$  are constant values, and  $L$  is the period of change  $\varepsilon_1$ , it is difficult to obtain analytical solution of the system of Eqs. (7). Because of that this system for this case was solved by numerical method of Runge–Kutta of fourth order. In Figure 5 dependences of diffraction efficiency of multi-layered hologram on wavelength under the following conditions:  $\lambda_0 = 0.55 \mu\text{m}$ ,  $\varphi = \theta_0 = 0.175 \text{ rad}$ ,  $n_0 = 1.52$ ,  $\Lambda = 1 \mu\text{m}$  are shown.

For holograms shown in Fig. 5, correlation of general thickness of hologram to the period  $L$  is 10:1, which leads to appearance of 8 peaks of small amplitude, placed between peaks of considerable amplitude. Since in decomposition of  $n_1(z)$  into Fourier complex series, as well as in  $\varepsilon_1(z)$ , there are only members of zero and  $\pm 1$  orders, we have in Fig. 5 only three strong peaks, the distance between which is defined by period  $L$ , peaks of higher orders are absent, contrary to Figs. 2 and 3, where those peaks are observed.

#### 4. Fabrication of multi-layered holograms

It is especially easy to record a two-layered hologram on photopolymeric materials [13] which have diffractive efficiency near 100% and resolution of more than  $6000 \text{ mm}^{-1}$ . Optical scheme of recording such a hologram is shown in Fig. 6a. The distance between holograms  $d$  is defined by the thickness of transparent glass substrate. At calibrated transparent substrates and calibrated thickness of photopolymeric material it is possible to record multi-layered hologram with  $m = 10$ , which for most applications is enough. It would seem possible to record multi-layered holograms using additional hologram according to Fig. 6b.

The analysis shows that spatial distribution of refractive index in photopolymer material according to Fig. 3b in the case of linear registration of interferometric picture can be expressed as follows:

$$n(x, y) = n_0 + n_{11} \sin\left(\frac{2\pi}{L}z\right) \cos\left(\frac{2\pi}{\Lambda}x\right) \quad (25)$$

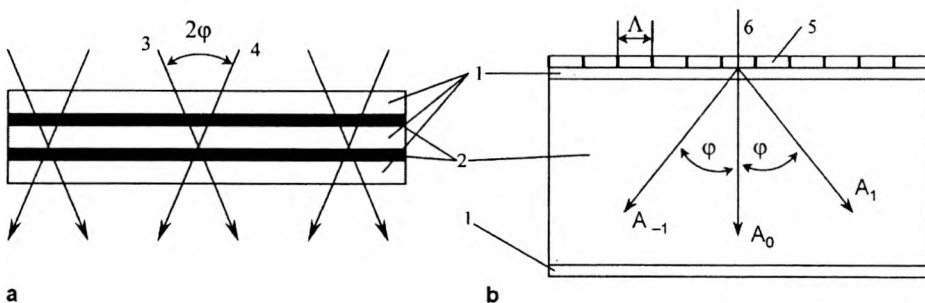


Fig. 6. Optical schemes of recording multi-layered holograms, 1 – glass substrate, 2 – photopolymer: a – two-layered hologram, 3, 4 – interference beams, b – multi-layered holograms, 5 – additional assisting hologram, 6 – coherent beam normal to additional hologram.

where  $L$  can be expressed using  $\Lambda$  and the wavelength  $\lambda_0$  of exposing light in the following form:

$$L = \frac{n_0 \Lambda^2 (1 + \sqrt{1 - \lambda_0^2 / n_0^2 \Lambda^2})}{\lambda_0} \quad (26)$$

If  $\lambda_0 \ll \Lambda$ , then formula (26) will become simpler and  $L \approx 2n_0 \Lambda^2 / \lambda_0$ . To obtain a dependence of diffraction efficiency on wavelength, as shown in Fig. 5a (in some cases this dependence is optimum for light show), condition  $\lambda_0 = 2n_0 / 25$  [ $\mu\text{m}$ ] has to be executed. At such a wavelength it is not possible to record a hologram on photopolymer composite. Besides, from formula (25) follows  $n_{10} = 0$ , and that is why central peak as in Fig. 5a will be absent.

In our opinion, multi-layered hologram on the thick substrate of photopolymer composite can be recorded by holographic method using three-multiple exposures on usual holographic scheme at the angle of meeting of two beams on photopolymer of  $2\varphi$ . First exposition is along symmetrical scheme when bisector of the angle  $2\varphi$  is normal to the surface of polymer. In the second and third exposures photopolymer between two glass plates turns to the small angle  $\pm\alpha$  from symmetrical placement at first exposure. In this case, after recording the refractive index is determined by the following formula:

$$n(x, z) = n_0 + n_{10} \cos\left(\frac{2\pi x}{\Lambda}\right) + n_{11} \sin\left(\frac{2\pi z}{L}\right) \cos\left(\frac{2\pi x}{\Lambda_1}\right) \quad (27)$$

When recording the hologram angles  $\alpha$  and  $\varphi$  and also the wavelength  $\lambda_0$  define  $L$ ,  $\Lambda$  and  $\Lambda_1$ , the following correlations being true:

$$\Lambda = \frac{\lambda_0}{2n_0 \sin \varphi},$$

$$L = \frac{\Lambda}{\sin \alpha},$$

$$\Lambda_1 = \frac{\Lambda}{\cos \alpha}.$$

If  $\alpha \ll 1$ , then  $\Lambda \approx \Lambda_1$ , and in our case when  $L/\Lambda = 25$ ,  $\varphi = 0.175$ ,  $\lambda_0 = 0.55$ , then  $\sin \alpha = 0.04$  and  $\cos \alpha = 0.9992$ , and scheme of recording of hologram with characteristics as in Fig. 5a could be realised.

## 5. Conclusions

As we could see, multi-layered holograms have interesting properties making them similar to Fabry-Perot interferometer, because in those holograms multi-beam

interference is present. Two-layered holograms are characterized by oscillation of the dependence of diffraction efficiency due to either of beam incidence onto the hologram, or on wavelength of incident beam. Besides, for every wavelength there could be found such an incident angle at which diffraction efficiency of hologram practically equals one. Such unique properties of multi-layered holograms could have some applications. In our opinion, among such applications the following are worthwhile to mention: sensors of small angle movements, dispersion element in tunable lasers, in systems of electric stabilisation of frequency of semiconductor lasers, in optical devices based on control of wave fronts, dispersion element for spectral devices, and also for grading of scales of those devices on wavelengths, and, finally in light show. Obviously, every application will require multi-layered hologram with that or other properties. For example, two-layered hologram with characteristics shown in Fig. 4 could be used as dispersion element for selection of wavelengths in lasers and as sensors of angle movement, for grading of scales of spectral devices it is better to use multi-layered hologram, characteristics of which are shown in Fig. 3b, and in light show it will be effective to apply of multi-layered holograms with characteristics shown in Fig. 3a and in Fig. 5. Also other applications will be possible.

## References

- [1] YAKYMOVYCH A.P., *Opt. Spectrosc.* **49** (1980), 158.
- [2] KOGELNIK H., *Bell Syst. Tech. J.* **48** (1969), 2909.
- [3] ZELDOVYCH B. YA., YAKOVLIEVA T.V., *Quantum Electron.* **11** (1984), 471.
- [4] ZELDOVYCH B. YA., MIROVICKIJ D.I., ROSTOVCEVA N.V., SEROV O.B., *Quantum Electron.* **11** (1984), 537.
- [5] DE FRE R., HESSELINK L., *J. Opt. Soc. Am. B* **11** (1994), 1800.
- [6] YARIV A., YEH P., *Optical Waves in Crystals*, Wiley, New York, 1984.
- [7] FITIO V. M., *Proc. SPIE* **4148** (2000), 34.
- [8] FITIO V. M., *Multilayered Volume Holograms and Their Properties*, Visnyk National University "Lvivska Polytechnica", Vol. 401, 2000, pp. 42–48.
- [9] LANDAU L. D., LIFSHIC YE. M., *Elektrodinamika sploshnykh sred*, Vol. VIII, [Ed] Nauka, Moscow 1982.
- [10] COLLIER R., BURCKHARDT C., LIN L. *Optical Holography*, Academic Press, New York, London 1971.
- [11] HANTMAKHER F. R. *Teoriya matric*, [Ed] Nauka, Moscow 1988.
- [12] YARIV A., *Quantum Electronics*, Wiley, New York, London, Sydney, Toronto, 1975.
- [13] SMIRNOVA T. N., GULNAZAROV E. S., TIKHONOV E. A., *Proc. SPIE* **1017** (1988), 190.

*Received August 16, 2001*